JOURNAL OF CATALYSIS 74, 282–295 (1982)

The Formation of Oxygen-Containing Organic Molecules by the Hydrogenation of Carbon Monoxide Using a Lanthanum Rhodate Catalyst

P. R. WATSON AND G. A. SOMORJAI

Materials and Molecular Research Division, Lawrence Berkeley Laboratory, and Department of Chemistry, University of California, Berkeley, California 94720

Received September 3, 1981; revised December 1, 1981

A $LaRhO_3$ catalyst was used for the hydrogenation of carbon monoxide at 6 atm pressure and between 225 and 375°C. The oxide is stable to reduction to the metal, but X-ray photoelectron and Auger spectroscopy studies show that the active catalyst contains a reactive carbonaceous layer with most of the rhodium in the 1+ oxidation state and with some metal present. The presence of large amounts of oxidized rhodium species correlates with the production of large quantities of oxygenated hydrocarbons up to 80+ wt%. The selectivity to different oxygenated products varies with temperature; yields of acetaldehyde and ethanol in excess of 50 wt% are found at temperatures around 300°C. The activation energies for the formation of all the products except methanol are similar at 28 ± 2 kcal/mole indicating that they are likely to form from a common CH_x precursor, obtained by dissociative adsorption of CO. Methanol is probably formed from molecular CO with an activation energy of 16 ± 3 kcal/mole. The changes in selectivity with temperature can be explained by competing carbonylation and hydrogenation reactions coupled with changing concentrations of molecular and dissociated CO on the surface.

1. INTRODUCTION

There is a widespread interest in the production of important oxygenated chemicals containing two carbon atoms, such as ethanol, acetic acid, and ethylene glycol, from nonpetroleum sources, in particular by the catalytic hydrogenation of carbon monoxide. Supported rhodium catalysts appear to be one of the most promising candidates for this purpose (*1–5*). However, different catalyst formulations lead to very different product distributions ranging from high yields of methanol and ethanol (*3, 4*) to acetaldehyde and acetic acid (*1, 2, 5*) or solely hydrocarbon products (*6*). It appears that the exact chemical environment and nature of the catalytically active rhodium species that are present on the surface of the catalyst vary considerably, depending upon the support and method of catalyst preparation in order to account for these drastic changes in catalytic behavior.

To investigate the origin of these fascinating behavioral differences between nominally similar rhodium catalyst systems, we have explored the characteristics of model, low-surface-area, unsupported rhodium catalysts for the hydrogenation of CO in the pressure range 1–10 atm (*7–9*). These studies are performed in such a manner that catalysts which are used at these moderate pressures that approach industrial conditions can be routinely monitored for changes in surface composition, structure, and oxidation state. Thus surface properties can be correlated with catalytic activity and selectivity more readily than for highly dispersed supported systems.

Studies on metallic rhodium single crystals and foils (*7, 8*) have shown that while clean elemental rhodium is a stable but mediocre methanation catalyst, preoxidation of the surface of a foil or crystal results in enhanced methanation activity and the formation of small amounts of oxygenated species. Most recently we have extended these studies to the rhodium–oxygen system in general (*8*). These investigations showed that the oxides of rhodium are ther-

0021-9517/82/040282-14$02.00/0

modynamically unstable under the reducing conditions of the synthesis reaction. However, it was uncovered that the dried hydrate of rhodium sesquioxide ($Rh_2O_3 \cdot 5H_2O$), while suffering some surface reduction, remained stable for hours and, importantly, produced up to 25+ wt% of oxygenated products (mainly acetaldehyde) at low conversion levels. The results of kinetic studies and gas-phase additive experiments (addition of ethylene) showed that the formation of these oxygenates results from CO insertion into C_xH_y surface species competing favorably with hydrogenation. This carbonylation ability appeared to be linked to the stabilization of at least some of the surface rhodium in a higher than zero oxidation state.

In order to prevent the reduction of the metal ions to the metallic state, we have incorporated rhodium ions into a stable oxide lattice, La_2O_3. This paper describes results obtained for the hydrogenation of CO at 6 atm pressure in the temperature range 225–375°C over lanthanum rhodate, $LaRhO_3$.

Our results show that this oxide is stable under these reaction conditions indefinitely, although change with time of the catalyst selectivity does occur. Large quantities of oxygenated products are observed ranging up to 80 wt% of the total product yield. Depending upon the experimental conditions, the major product can be methanol, ethanol, or acetaldehyde as a result of the shift in the surface concentrations of various reaction intermediates under different reaction conditions. We compare these results with those from supported catalyst systems, particularly those using lanthanum oxide as a support, and discuss the significance of the rhodium oxidation state as a determinant of the product distribution.

2. EXPERIMENTAL

The experimental apparatus, described in detail elsewhere (*7, 10*), consists of an ultrahigh-vacuum chamber pumped with ion and diffusion pumps and equipped with retarding-field LEED/Auger optics, a mass spectrometer, and an internal high-pressure (<20 atm) isolation cell. With the cell open, samples can be cleaned by argon ion sputtering, annealing, or chemical treatments with gases admitted via a leak valve. Surface composition was monitored regularly by Auger electron spectroscopy (AES). With the cell closed, the apparatus was operated as a stirred batch reactor. The CO (Matheson 99.95%) was passed through a copper tube heated to ~200°C and then through a molecular sieve chilled by an acetone–dry ice bath to remove carbonyls; the H_2 (Liquid Carbonic 99.95%) was used without further purification. Reaction products were monitored gas chromatographically as described elsewhere (*9*).

X-Ray photoelectron spectroscopy (XPS) measurements were carried out in a separate instrument with no provision for sample treatment (*9*). Binding energies were referenced to C 1*s* at 285.0 eV.

High-pressure CO hydrogenation reactions were carried out over $LaRhO_3$ samples which were deposited as thin layers from a methanol slurry onto gold foils. The metal foil provided both the mechanical support for these powder samples and a means of heating. The foils were heated resistively both to outgas the samples and to establish reaction temperatures which were measured by an Alumel–Chromel thermocouple attached to the foil.

Lanthanum rhodate was prepared by grinding together stoichiometric quantities of $Rh_2O_3 \cdot 5H_2O$ (Alfa Products, 95+%) and La_2O_3 (Lindsay Chemical Co. 99.99%), and heating at 1100°C in air in a platinum crucible (*11*) to form a grey–black powder. Lanthanum rhodate has a distorted perovskite structure (*11*).

3. RESULTS

3.1. Auger and Photoelectron Spectroscopy Studies of $LaRhO_3$ and Thermal Desorption of CO and D_2

Spectroscopic studies of $LaRhO_3$ appear

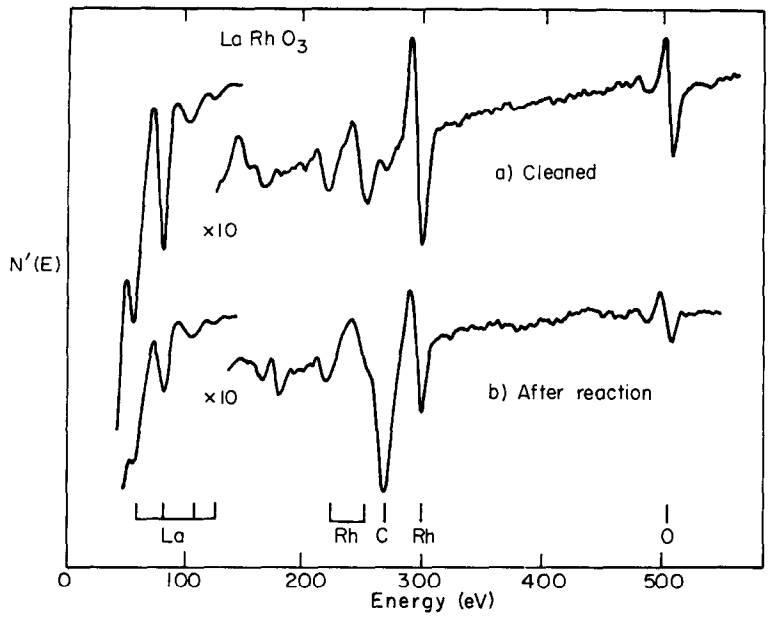

FIG. 1. Auger electron spectra, taken with a retarding-field analyzer, of $LaRhO_3$ at 1.5 kV primary energy and 10 μA beam current: (a) cleaned by heating to 400°C for 1 hr followed by argon ion bombardment (5 μA, 500 eV) for 15 min; (b) the same sample after reaction in 1 : 1 H_2/CO at 6 atm and 350°C for 2 hr.

to be lacking in the literature, although the closely related $LaCoO_3$ has received some attention (*12*). In Fig. 1 we present Auger electron spectra for a cleaned sample of $LaRhO_3$ that was subsequently used for a synthesis reaction in 1 : 1 H_2/CO and then reexamined spectroscopically. The spectrum of the cleaned surface shows four peaks at low energies (56, 78, 106, and 120 eV) that can be attributed to La transitions and are in reasonable agreement with literature values for lanthanum metal (*13*). The cleaned surface shows the usual triplet of major Rh transitions and an O^{515} peak with an intensity ratio of $O^{515}/Rh^{302} = 0.56$. After a synthesis reaction, (Fig. 1b) the major La, Rh, and O features are all reduced in intensity due to the deposition of a considerable quantity of carbon on the surface, evidenced by a very large carbon Auger peak. The O^{515}/Rh^{302} peak ratio has decreased only slightly to 0.43 indicating the stability of this oxide system even in the reducing atmosphere of the synthesis reaction. A small peak at 182 eV indicates that a small amount of Cl has diffused to the catalyst surface during reaction.

Heating the sample that had been reacted in 1 : 1 H_2/CO to 400°C leads to the evolution of a small amount of CO (detected by the mass spectrometer), but no visible diminution in the size of the carbon Auger peak. Heating to >450°C leads to the massive evolution of CO and CO_2 due to abstraction of lattice oxygen as noted for Rh_2O_3 (*9*). Hence, the carbonaceous layer that is deposited during reaction appears to not be adsorbed CO, but to be of the active type seen previously on Rh (*7–9*), Ni (*14–16*), and Fe (*17–19*) catalysts.

The Rh XPS binding energies for used and fresh $LaRhO_3$ are collected in Table 1 together with literature data for rhodium metal and Rh^+ and Rh^{3+} compounds. The fresh $LaRhO_3$ shows a rather sharp Rh $3d_{5/2}$ line at a binding energy of 311.0 eV, a value which agrees well with the literature data for Rh^{3+} compounds. After reaction, the Rh

TABLE 1

XPS Binding Energy (E_B) Data for Rh $3d_{5/2}$ Line Relative to C 1*s* at 285.0 eV

Sample	E_B (eV)	ΔE_B (eV)	Ref.
Rh	307.1	—	(*20, 21*)
Rh^+ compounds	307.6–309.6	—	(*22*)
	(308.8)[a]		
Rh^{3+} compounds	308.8–311.3	—	(*22*)
	(310.3)[b]		
$LaRhO_3$	311.0	2.0	This work
Used $LaRhO_3$	307.7	2.7	

Note: ΔE_B represents the full width at half-height.
[a] Mean E_B for 16 compounds.
[b] Mean E_B for 48 compounds.

3*d* XPS lines are considerably broader and shifted to a value of 307.7 eV. This is at the low end of the range for Rh^+ compounds compiled by Nefedov (*22*). Therefore, it appears that the working $LaRhO_3$ catalyst has an average oxidation state close to 1. However, the breadth of the line in the used catalyst suggests that the catalyst surface contains a mixture of oxidation states, probably consisting mainly of Rh^0 and Rh^+.

In Fig. 2 we present thermal desorption spectra (TDS) of CO and D_2 from the fresh oxide and the same sample after reaction. We see that CO desorbs from the fresh oxide in a single, broad peak centered at around 225°C; on the used catalyst CO now shows two desorption peaks at 150 and 272°C, respectively. The D_2 desorption peak from the fresh $LaRhO_3$ sample is at 177°C and drops dramatically to 104°C on the used catalyst, though a shoulder remains at higher temperatures.

In order to obtain a clearer picture of what these TDS results represent, we have converted these peak temperatures to heats of desorption and compared them in Fig. 3 with previous results for a used rhodium oxide catalyst (*9*), literature data for rhodium metal (*7, 23–26*), and data measured during this study for La_2O_3. First-order kinetics are assumed for the CO data, second order for H_2, and a preexponential factor of 10^{14}.

At the top of Fig. 3 we immediately note the similarity of the desorption spectra from La_2O_3 and fresh $LaRhO_3$ with D_2 desorbing with a heat of desorption of about 28 kcal/mole and CO about 32 kcal/mole. This high heat of desorption for D_2 is pre-

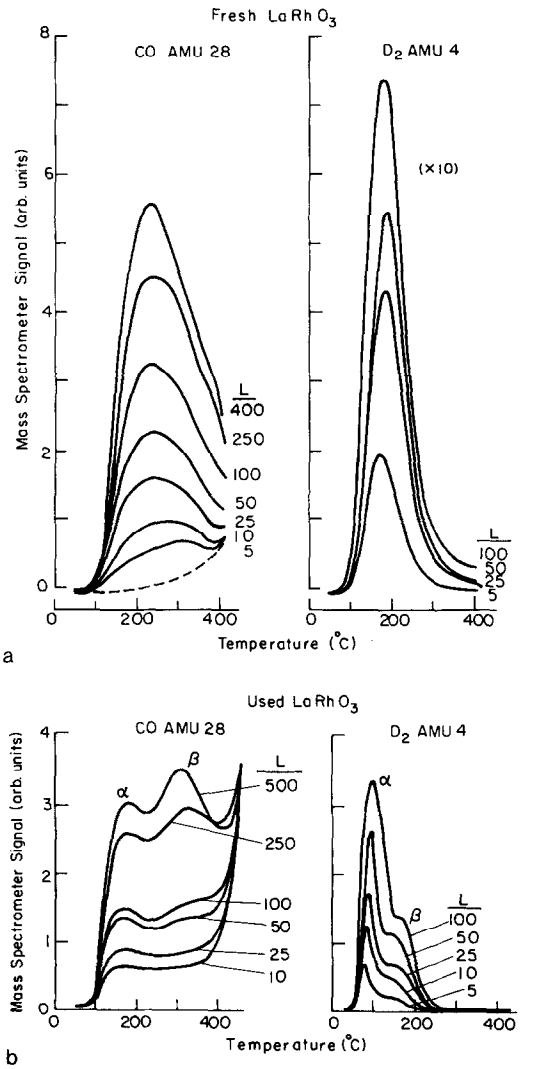

FIG. 2. Thermal desorption spectra of CO and D_2 from (a) a freshly cleaned $LaRhO_3$ surface, and (b) the same surface that has been used as a catalyst in 1 : 1 H_2/CO at 350°C, 6 atm for 4 hr.

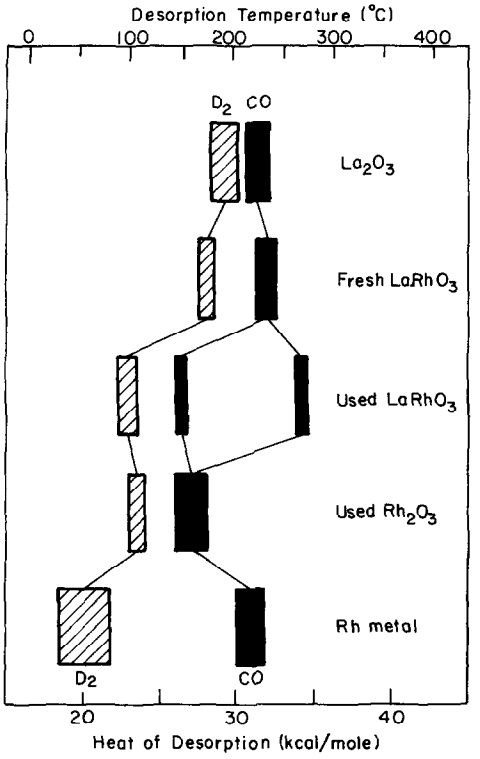

FIG. 3. Heat of desorption (kcal/mole) of CO and D_2 from La_2O_3, fresh and used $LaRhO_3$ (this work), used rhodium oxide (*9*), and rhodium metal (*7, 23–26*). The spread of each value represents the variation with surface coverage rather than experimental uncertainty.

sumably due to hydroxyl formation upon adsorption; desorption can then only be achieved by breaking relatively strong O–D bonds (102–111 kcal/mole for H_2O). The adsorption of CO on La_2O_3 appears to be little documented in the literature. What seems clear from our data is that CO is stabilized only slightly by including Rh^{3+} in the crystal lattice instead of the presence of metallic rhodium.

Starting from the bottom of Fig. 3, we see that relative to rhodium metal, D_2 desorbs at a higher temperature and CO at a lower temperature on dried $Rh_2O_3 \cdot 5H_2O$ that has been used for CO hydrogenation (used Rh_2O_3 in Fig. 3), as detailed in Ref. (*9*). The used $LaRhO_3$ sample appears to resemble used Rh_2O_3 in the desorption of D_2; the heat of desorption increases smoothly from metallic rhodium through used Rh_2O_3, which is known to be partially reduced (*9*), used $LaRhO_3$, to fresh $LaRhO_3$ and La_2O_3. Used $LaRhO_3$ shows two CO binding states, one of which appears to correlate with CO desorption from the fresh oxide except shifted to an even higher heat of desorption of 33 kcal/mole. This change in CO desorption behavior on the used catalyst may be a result of the carbonaceous layer deposited during reaction detected by Auger spectroscopy, or may reflect the change in oxidation state of the rhodium at the catalyst surface. It is hoped that further studies may help to separate these effects.

3.2. Product Distributions

The accumulation of products with time for a reaction carried out at 225°C over a freshly prepared $LaRhO_3$ surface is shown in Fig. 4. Under this set of reaction conditions, methanol, methane, and C_2 oxygenates are the major products with only smaller amounts of higher hydrocarbons, which are almost exclusively alkenes. Un-

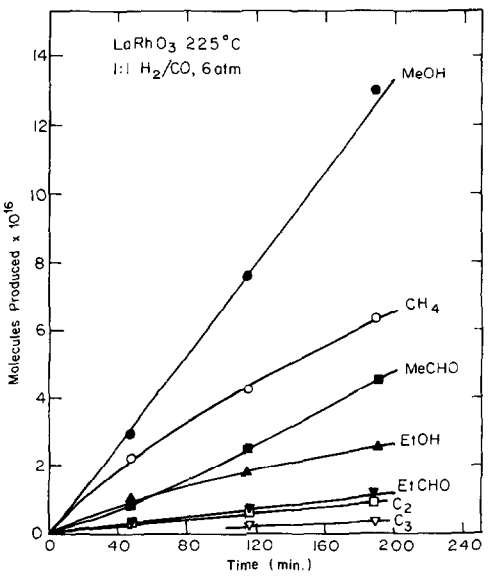

FIG. 4. Accumulation of products with time for the reaction of 1:1 H_2/CO at 6 atm and 225°C over $LaRhO_3$.

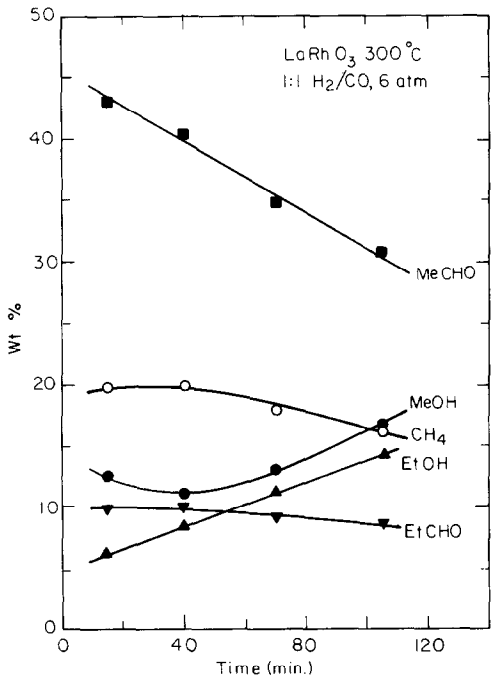

FIG. 5. The change in product distribution (in wt%) with time for the major products of the reaction of 1 : 1 H_2/CO at 6 atm and 300°C over $LaRhO_3$. The balance consists of ethylene, propylene, and smaller amounts of higher oxygenates.

der these conditions the relative amounts of the various products do not alter significantly with time, but at higher temperatures interesting effects are seen, as demonstrated in Fig. 5. When the reaction temperature is increased to 300°C the oxygenated compounds, in particular those containing two carbon atoms, dominate the product spectrum; the balance of products not shown in this figure (about 10 wt%) is mainly C_2 and C_3 alkenes and smaller amounts of higher aldehydes and alcohols. La_2O_3 is catalytically inactive under these conditions as noted by Ichikawa (*3*). An important feature of this diagram is the variation of the relative quantities of some of the products with time: MeCHO/EtOH, in particular, appears to show a mirror image or compensation effect. Initially acetaldehyde is the major oxygenated product (43 wt%), while ethanol is only a minor product (6 wt%) at 300°C. As the reaction proceeds, we notice a smooth decrease in the amount of acetaldehyde and a simultaneous increase in the ethanol yield such that the sum of the two stays constant at 47 ± 3 wt%.

The origin of the remarkable change of the MeCHO/EtOH yields is due to a slow alteration in the nature of the catalyst surface with time. The data shown in Fig. 6 clearly show this. The reaction was carried out at a higher temperature than the data of Fig. 5, but a similar trend is apparent. The ratio of MeCHO : EtOH drops from about 6 : 1 to less than 2 : 1 in 90 min. After replenishment of the reactants, ethanol production resumes at essentially the same rate as at the end of the initial reaction; the acetaldehyde production resumes at a somewhat higher rate, but substantially less than its starting value. Thus the gradual change in product distribution is not linked to post-reaction events such as secondary hydrogenation of acetaldehyde but is due to a change in the relative rates of formation of acetaldehyde and ethanol. This, therefore, is clear evidence for a catalyst aging process.

Additional evidence is shown in the third section of Fig. 6. Here the sample has been treated by heating in oxygen (450°C, 1×10^{-5} Torr, 5 min) and ion bombardment (500 eV, 5 μA for 30 min) until clean apart from a small amount of residual carbon and the reaction begun again. Here we note a reversion to the initial behavior with a very low production of ethanol which later grows. Clearly, the cleaning process has removed some or all of the aged surface material exposing fresh catalytic sites which themselves age at a rate similar to the fresh catalyst. Whether the important process is removal of the accumulated carbon layer or exposure of new rhodium sites is not yet clear.

The variation of the product distribution obtained at 300°C and several values of the H_2/CO ratio is shown in Fig. 7. The effect of changing this parameter is small. There is an increase in the production of methane

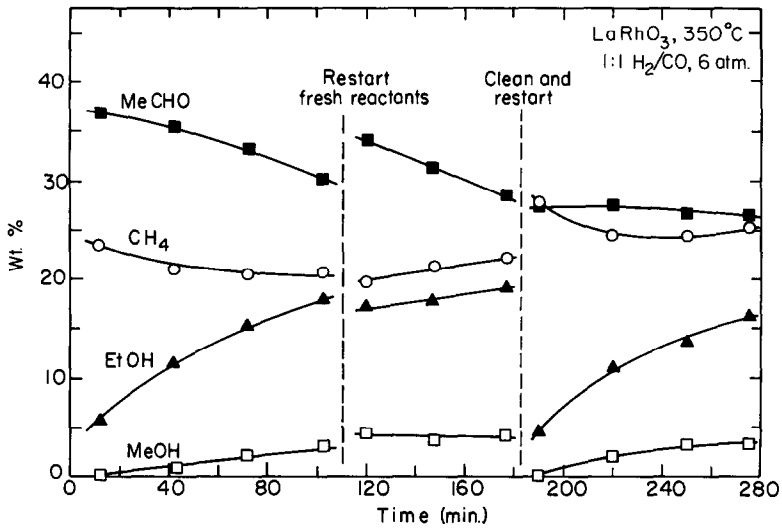

FIG. 6. The change in product distribution with time for the production of acetaldehyde/ethanol, methane, and methanol from 1:1 H_2/CO at 6 atm and 350°C over $LaRhO_3$ showing the effect of replenishing the reactants and cleaning the sample (450°C in 1×10^{-5} Torr O_2 for 5 min followed by Ar^+ bombardment, 5 μA, 500 eV for 30 min) and using fresh reactants.

at high H_2/CO ratios, presumably due to a relatively high rate of hydrogenation compared to chain growth. The figure also illustrates the large quantities of oxygenated products that are formed over this catalyst. At 300°C, the total yield of oxygenates is 80 wt% with most of this (>50 wt%) made of C_2 oxygenates, these being acetaldehyde and ethanol. Only very small traces of acetic acid and its esters were ever detected.

The variation of product distribution with temperature, depicted in Fig. 8, is much more dramatic, however. Here are plotted the major reaction products over the temperature range 225–375°C. The curves drawn through the points are merely a guide and are not intended to represent a fit of the data points. There are three distinguishable regions of activity. At low temperatures, around 225°C or less, methanol production becomes increasingly important, whereas at high temperatures, 350°C and higher, methane predominates. However, at intermediate temperatures (250–325°C) C_2 oxygenate products are most abundant and are most favored at temperatures close to 300°C. We shall return to discussion of this diagram in Section 4.

In Table 2 we compare the results obtained in this work at 225 and 300°C with those reported for $Rh_2O_3 \cdot 5H_2O$ (*9*), those of Ichikawa (*3*) for a La_2O_3-supported rhodium catalyst, and those of Union Carbide (*1, 2*) and Hoescht (*5*) workers for silica-supported rhodium. We quote both initial and approximate steady-state distributions. Our low-temperature product distribution compares favorably with that reported by Ichikawa (*3*) for a Rh/La_2O_3-supported catalyst if we allow for a more complete hydrogenation of acetaldehyde to ethanol in Ichikawa's case. At the higher temperature we see that $LaRhO_3$ shows a great improvement in performance over $Rh_2O_3 \cdot 5H_2O$ (*9*) showing a large drop in hydrocarbon formation accompanied by a very large increase in the total oxygenate production. These initial higher-temperature results compare favorably with those of Wilson and co-workers (*1, 2*) for silica-supported rhodium, and approach those disclosed in patent form only by German workers (*5*) if we allow for greater oxidation to acetic acid in these cases.

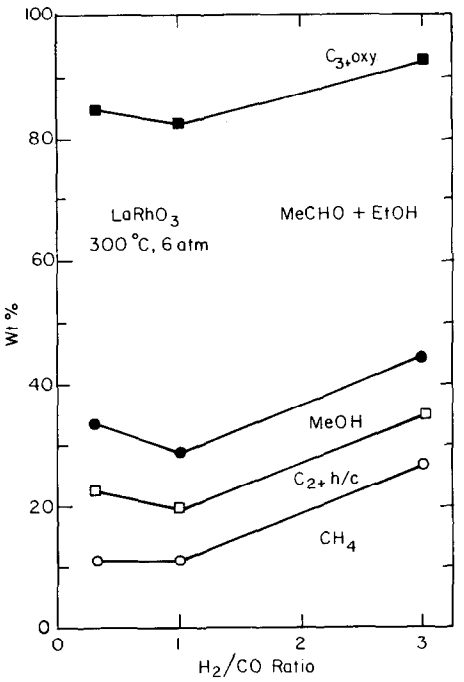

FIG. 7. The effect of changing the H_2/CO ratio on the reaction over $LaRhO_3$ at 6 atm and 300°C.

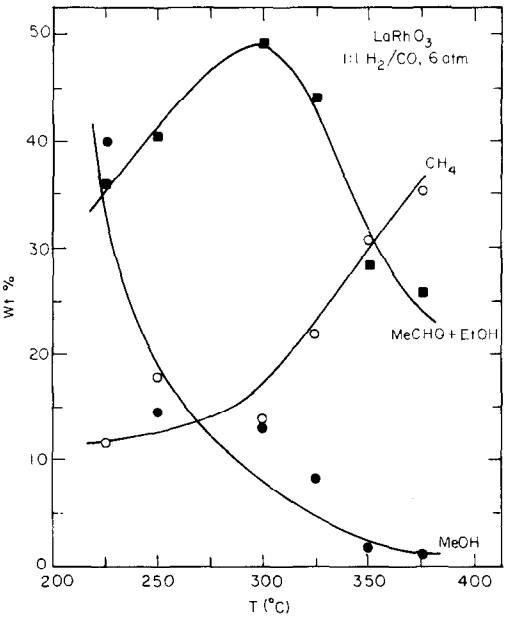

FIG. 8. The effect of changing the temperature on the production of CH_3CHO + C_2H_5OH, CH_4, and CH_3OH over $LaRhO_3$ at 6 atm and 1 : 1 H_2/CO ratio.

3.3 Kinetics

We have measured both rates and energies of activation for the hydrogenation of CO over $LaRhO_3$. In Table 3 we display the rate of formation of products and of consumption of CO at two different temperatures; these numbers are also quoted on a per gram of catalyst basis for compari-

TABLE 2

Product Distribution for CO Hydrogenation over Various Rhodium Catalysts

Catalyst	T (°C)	P (atm)	H_2/CO	Product distribution (wt%)						Ref.
				C_1	C_{2+}	MeOH	EtOH	MeCHO	MeCOOH	
$LaRhO_3$	225	6	1	16	7	33	19	15	0	This work[a]
				12	6	40	13	23	0	This work[b]
Rh/La_2O_3	225	0.1	2	23	2	30	46	Trace	0	(*3*)
$LaRhO_3$	300	6	1	20	8	12	6	43	0	This work[a]
				16	9	17	14	31	0	This work[b]
Rh_2O_3	300	6	1	39	46	3	Trace	15	0	(*9*)
Rh/SiO_2	300	70	1	53	4	0	Trace	30	6	(*1*, *2*)
Rh/SiO_2	300	80	1	9	[c]	[c]	4	42	37	5[d]

[a] Initial product distribution.
[b] Approximate steady-state product distribution.
[c] Not reported.
[d] In mole percentage.

TABLE 3

Kinetic Results for the Hydrogenation of CO over $LaRhO_3$ at 6 atm, 1 : 1 H_2/CO

T (°C)	Product	Rate of formation[a]		
		$\times 10^{14}$ molecules/s	$\times 10^{17}$ molecules/hr	$\times 10^{-1}$ g/g $LaRhO_3$/hr
300	CH_4	1.18	4.25	0.11
	C_2H_4	0.21	0.76	0.03
	CH_3OH	0.83	2.99	0.16
	C_2H_5OH	0.53	1.91	0.15
	CH_3CHO	0.83	2.99	0.22
	C_2H_5CHO	0.30	1.08	0.10
Total CO consumed[b]		6.77	24.37	1.13
375	CH_4	52.70	189.72	5.04
	C_2H_4	8.35	30.06	1.40
	CH_3OH	2.77	9.97	0.53
	C_2H_5OH	9.37	33.73	2.58
	CH_3CHO	11.80	42.48	3.10
	C_2H_5CHO	5.52	19.87	1.91
Total CO consumed[b]		164.28	591.41	27.51

[a] CH_3CHO and C_2H_5OH rates are after 2 hr of reaction.
[b] Ignoring CO_2 formation.

son purposes. This was done because no *in situ* determination of surface area and the number of surface rhodium atoms was available.

The data of Table 3 immediately allow us to ascertain that the reaction is truly catalytic and not merely stoichiometric, and that the oxygen in the oxygenated products arises from CO and not lattice oxygen. A typical sample of $LaRhO_3$ weighs about 1–2 mg which corresponds to roughly 2×10^{18} molecules of $LaRhO_3$. If all the Rh atoms were on the surface of the catalyst then a CO molecule would be reacted about every 25–500 s on each rhodium atom. If the reaction were merely stoichiometric it would cease after only 1000 s at most. However, as was shown in Figs. 4–6, the reaction can be continued for hours with little diminution in the rate of product formation. Therefore, every site must be turning over many CO molecules to products and the reaction is truly catalytic.

To determine whether the oxygen in the oxygenated hydrocarbon products arises from CO or lattice oxygen, we can compare the number of oxygen atoms available in the lattice with the number appearing in the products of reaction. In a typical $LaRhO_3$ sample there are about 6×10^{18} oxygen atoms. Now, using the 300°C data of Table 3, roughly 2×10^{18} oxygen atoms appear in the products per hour and many more at higher temperatures (1×10^{19}/hr at 375°C). Actually this total is low due to the neglect of formation of H_2O and CO_2 which are not detected. Therefore, as the reaction can be carried on for several hours with no drop in the production of oxygenated compounds, we can conclude that oxygen atoms from CO are, in fact, appearing in the oxygenated products, although participation by lattice oxygen through exchange with CO is possible.

In Table 4 we list the activation energies deduced from the Arrhenius equation for

TABLE 4

Energies of Activation for the Formation of Various Products of the Reaction of H_2 and CO over Rhodium Catalysts

	CH_4	C_2H_4	MeOH	EtOH	MeCHO	EtCHO	Ref.
$LaRhO_3$[a]	27 ± 2	27 ± 2	16 ± 3	26 ± 2	28 ± 2	29 ± 2	This work
Rh_2O_3[a]	26 ± 2	26 ± 2	16 ± 4	—	26 ± 2	—	(9)
Rh/La_2O_3[b]	28	—	12	20	—	—	(3, 4)

[a] 1:1 H_2/CO, 6 atm.
[b] 2:1 H_2/CO, 0.1 atm.

the major products of this reaction and compare them with earlier data for rhodium oxide (9) and Rh/La_2O_3 (3, 4). We can see that on $LaRhO_3$ all the major products, with the exception of methanol, have essentially the same energy of activation within experimental error of 26–28 kcal/mole. The results on the supported catalyst (3, 4) are very similar for methane at 28 kcal/mole, but rather different for ethanol at 20 kcal/mole. The values of the activation energy found here for methane agree well with those reported earlier for rhodium catalysts of about 24 kcal/mole (1, 2, 6–8), and for methanation on Fe (6, 17) (27 kcal/mole), and Ni (6, 16) (25 kcal/mole) catalysts. Both the supported catalyst and rhodium oxide data agree with our $LaRhO_3$ results in describing the activation energy for methanol formation as being substantially lower at ~16 kcal/mole. This presumably reflects a different reaction mechanism and will be discussed in the following section.

4. DISCUSSION

4.1. Reaction Mechanism

The kinetic results presented in the last section indicate that we are dealing with two competing reaction mechanisms—one which gives rise to the formation of methanol with an activation energy of about 16 kcal/mole and a second which results in the formation of all the other products with the same activation energy of about 28 kcal/mole.

The similarity of the activation energies for the formation of all products, with the exception of methanol, implies a common precursor and rate-determining step. The closeness of this value to those reported for methanation catalysts (1, 2, 6–8) suggests that this rate-determining step is the same as that for methanation. This step has been postulated to be formation of a surface CH_x species by many workers (1, 2, 7, 8, 14–19, 34) for methanation on Ni, Fe, Ru, and Rh; it is not clear, however, whether CO dissociation or subsequent hydrogenation is rate limiting. While evidence for CO dissociation on Fe and Ni is strong (14, 19), such dissociation is less marked on rhodium, but does occur at temperatures in the range employed in our work (7, 24, 27). This carbonaceous layer is reactive and can be hydrogenated in pure H_2 after a synthesis reaction to yield solely hydrocarbons. During this experiment no oxygenated products are detected, indicating that this layer contains no strongly bound oxygenated species.

After formation of such a CH_x species, reaction could proceed by hydrogenation to CH_4, CO insertion to yield CH_3CHO or C_2H_5OH, and chain growth by insertion and hydrogenation or by polymerization of CH_x species. The large preponderance of oxygenated products that we observe suggests that on $LaRhO_3$ carbonylation competes favorably with hydrogenation, a phenomenon well noted in hydroformylation reactions using rhodium catalysts (28–30), and seen clearly on rhodium oxide (9).

Methanol formation appears to occur by a different reaction mechanism with a much lower activation energy. On oxide catalysts the methanol synthesis mechanism has usually been assumed to be nondissociative (*31*). On supported metal catalysts (Pt, Pd, Ir) (*32*), the reaction mechanism also appears to proceed through nondissociated CO; most recently isotopic studies by Takeuchi and Katzer (*33*) have established such a route for the formation of methanol on Rh/TiO_2. Hence, we propose that methanol formation proceeds through a direct hydrogenation of chemisorbed CO on $LaRhO_3$. Thermodynamically, methanol will be favored at lower temperatures (not accessible in this study due to insufficient activity) and higher pressures.

If we reexamine the data of Fig. 8 we can now divide the CO hydrogenation reaction of $LaRhO_3$ into three temperature regions in which different reactions are dominant. At temperatures <225°C methanol production through chemisorbed CO predominates with E_a = 16 kcal/mole. At higher temperatures, this reaction is superseded by a dissociative adsorption of CO to produce CH_x species (E_a = 26–28 kcal/mole) which can then follow parallel paths of CO insertion to produce oxygenates or hydrogenation to methane. At the highest temperatures studied, methanol production is severely depressed, while methane is the major product. At intermediate temperatures, CO insertion competes favorably with hydrogenation resulting in a maximum yield of C_2 oxygenates at temperatures close to 300°C. This reaction scheme is summarized as:

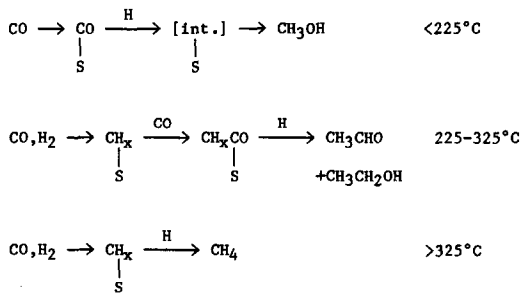

We cannot rationalize the shape of these curves shown in Fig. 8 solely in terms of the rate-limiting kinetic steps that are responsible for the measured activation energies. If we base our arguments solely on these values then we would indeed predict a relative decrease in methanol yield with temperature, but the similarity of the measured activation energies for the other products might lead us to predict a similar increase for each product with temperature, in contrast to the behavior observed. We can overcome this apparent contradiction if we recall, however, that the experimental activation energy is a measure of the degree of change of the reaction rate with temperature, but does not tell us anything about the absolute rates of formation of products that depend on both the activation energy and the preexponential factor. An examination of Table 3 shows that the absolute rate of production of methane increases by a factor of nearly 45 on increasing the temperature from 300 to 375°C, while the corresponding value for acetaldehyde formation is only a factor of 14. Thus the relative yield of acetaldehyde to methane depends on the absolute rates of formation at any given temperature. Thus, both the activation energy and preexponential factor are important in determining the product distribution.

In our model, all products other than methanol proceed from a rate-determining common precursor via parallel reaction paths. The relative amount of each product will depend upon the ability of an adsorbed reactant or intermediate to find a suitable reaction site and the relative concentration of the reactants needed for a particular reaction sequence, e.g., CO for insertion or H for hydrogenation, that are available on the surface. The surface temperature will play a role in determining the populations of CO and H and the mobility of adsorbed species.

If we reexamine the thermal desorption results for CO and D_2 on used $LaRhO_3$ of Figs. 2b and 3, we can see that *in vacuo* H_2 could not compete effectively with CO for adsorption sites at typical reaction temper-

atures. However, the high partial pressure of hydrogen under reaction conditions must ensure some surface hydrogen concentration, even at surface temperatures in excess of its temperature of maximum desorption rate.

At low temperatures we can expect much of the adsorbed CO to populate both CO states in the used catalyst TDS spectrum, but relatively little of this will be dissociated below 300°C (*7, 27*), and hence we can expect methanol production to be dominant. As the temperature is raised, more CO will dissociate, while nondissociated CO will become more mobile, leading to increased CH_4 and oxygenate yields but lower methanol yields. At the highest temperatures sufficient CO is probably dissociated that large islands of carbonaceous material form which present many sites for hydrogenation to methane, but CO insertion is markedly reduced. Thus a maximum in C_2 oxygenate production is seen when the relative effects of CO dissociation, CO insertion, and hydrogenation are balanced correctly.

4.2. The Nature of the Catalytic Surface

The results of the electron spectroscopic experiments show that the composition of the catalyst surface changes during the course of the reaction. A layer of a reactive carbonaceous deposit builds up on the catalyst surface while the average oxidation state of rhodium drops from 3 in the fresh oxide to close to 1 in the used catalyst. At the same time no great loss of oxygen from the surface occurs; incorporation of rhodium ions into the refractory La_2O_3 lattice has clearly decreased the tendency to reduction when compared to metastable Rh_2O_3 (*9*). These changes profoundly affect the binding energy of CO and D_2 on the surface. At this time, it is difficult to separate the influence of the two effects on the selectivity changes noted earlier.

The picture of the nature of the catalyst surface that is emerging from the spectroscopic and kinetic results is that the catalysis on this type of surface requires several sites. The reactants and intermediates migrate from place to place on the catalyst surface during their residence time and undergo different reactions at sites of differing chemical nature and reactivity.

Thus we know from previous studies (*7, 8*) that metallic rhodium will freely catalyze the formation of methane, presumably through a CO dissociative mechanism. With rhodium oxide (*9*), which exhibits either a mixture of high and low rhodium oxidation states or one slightly positive oxidation state, only modest amounts of oxygenated products are formed. The present work with $LaRhO_3$ shows that much of the rhodium in this catalyst is definitely in a nonzero oxidation state. The most plausible explanation is that most of the surface contains Rh^+ species with some small fraction close to Rh^0. Moreover this catalyst produces a high yield of two-carbon oxygenated chemicals. Hence it is attractive to associate the oxygenate-producing capabilities of these rhodium catalysts with the presence of a substantial amount of oxidized rhodium species on the surface.

Support for these ideas comes from recent infrared and XPS studies of supported rhodium catalysts which show that nominally reduced rhodium-loaded catalysts do contain oxidized rhodium species (*35, 36*) which may contribute to the catalytic activity. It has been suggested that surface hydroxyls on the support are effective in converting Rh^0 to Rh^+ (*37*). We can model the catalytic process by assuming that both oxidized and reduced forms of rhodium are needed to perform different types of chemistry. Thus reduced metal sites efficiently dissociate CO to form a CH_x intermediate which is either hydrogenated *in situ* or migrates to an oxidized rhodium site where CO insertion takes place. Such reactions are well known in rhodium oxo chemistry; in particular, the carbonylation of methanol, using iodide co-catalyst both homogeneously and heterogeneously (*29, 30*), is thought to proceed through CO insertion

reactions where oxidized rhodium species are implicated as active centers. After the insertion reaction has occurred the surface intermediate can desorb as acetaldehyde or migrate to a suitable hydrogenation site (probably metallic) to eventually emerge as ethanol.

Our results show the value of studying relatively simple and well-defined model CO hydrogenation catalysts under realistic conditions, but with the advantages of *in situ* surface characterization. Stabilizing an oxidized form of rhodium in a nonreducible oxide lattice enables a high selectivity to especially C_2 oxygenated products. On the other hand, reduced rhodium metal is a relatively good methanation catalyst, evidently through a dissociated CO route with efficient subsequent hydrogenation. Thus it is probable that some reduced metal is needed to initiate CO dissociation and chain growth while oxidized rhodium ion readily induces carbonylation. Thus the catalyst that is active for producing two carbon atoms containing oxygenated molecules must have both rhodium metal and rhodium ion sites.

There is a great deal of value, it seems, in stabilizing the transition metal ions in higher oxidation states by incorporating them into the stable crystal lattices of refractory oxides. This way a better control of the product distribution during CO hydrogenation can be achieved.

5. CONCLUSIONS

1. Lanthanum rhodate is a stable catalyst for the hydrogenation of CO at temperatures in the range 225–375°C at 6 atm pressure.

2. Rates of consumption of CO of 2.75 g CO/g $LaRhO_3$/hr can be achieved. Methanol has an activation energy of formation of 16 ± 3 kcal/mole, while all the other major products (methane, acetaldehyde, and ethanol) are formed with activation energies of 28 ± 2 kcal/mole.

3. Large quantities of oxygenated products are formed, up to 80+ wt%. The product distribution varies with temperature in a way that can be separated into three regimes: (a) ≤ 225°C—methanol production dominates; (b) >350°C—methane is the major product; (c) in the intermediate range 225–350°C production of acetaldehyde and ethanol is dominant and is maximized at about 50 wt% near 300°C.

4. The product distributions and kinetics can be accommodated with a reaction mechanism that involves an associative adsorption of CO to form methanol and a dissociative mechanism for the other products. The variation of selectivity with temperature is due to competing processes of hydrogenation and carbonylation and varying concentrations of molecular and dissociated CO and hydrogen on the surface.

5. Auger and XPS experiments reveal that the catalyst surface, after reaction, contains a reactive carbonaceous layer and a mixture of oxidized (probably Rh^+) and reduced rhodium species. TDS experiments reveal marked changes in the binding of CO and H_2 to the catalyst surface before and after reaction, which are linked to time-dependent changes in catalyst selectivity.

ACKNOWLEDGMENTS

This work was supported by the Director, Office of Energy Research, Office of Basic Energy Sciences, Chemical Sciences Division of the U.S. Department of Energy under Contract W-7504-ENG-48. We would like to thank Dr. R. Dodd for taking the XPS measurements.

REFERENCES

1. Ellgen, P. C., Bartley, W. J., Bhasin, M. M., and Wilson, T. P., *Advan. Chem. Ser.* **178,** 147 (1979).
2. Bhasin, M. M., Bartley, W. J., Ellgen, P. C., and Wilson, T. P., *J. Catal.* **54,** 120 (1978).
3. Ichikawa, M., *Bull. Chem. Soc. Japan* **51,** 2268, 2273 (1978).
4. Ichikawa, M., *J. Catal.* **56,** 127 (1979).
5. Wunder, F., Arpe, H. J., Leupold, E. I., and Schmidt, H. J., U.S. Patent 4,224,236 (Hoescht AC).
6. Vannice, M. A., *J. Catal.* **37,** 449 (1975).
7. Sexton, B. A., and Somorjai, G. A., *J. Catal.* **46,** 167 (1977).

8. Castner, D. G., Blackadar, R. L., and Somorjai, G. A., *J. Catal.* **66,** 257 (1980).
9. Watson, P. R., and Somorjai, G. A., *J. Catal.* **72,** 347 (1982).
10. Blakely, D. W., Kozak, E. I., Sexton, B. A., and Somorjai, G. A., *J. Vac. Sci. Technol.* **13,** 1091 (1976).
11. Wold, A., Post, B., and Banks, E., *J. Amer. Chem. Soc.* **79,** 6365 (1957).
12. Richter, L., Bader, S. P., and Brodsky, M. B., *Phys. Rev. B* **22,** 3059 (1980) and references therein.
13. "Handbook of Auger Electron Spectroscopy." Physical Electronics Industries, Inc., Edina, Minn.
14. Wentrec, P. R., Wood, B. J., and Wise, H., *J. Catal.* **43,** 363 (1976).
15. Araki, M., and Ponec, V., *J. Catal.* **44,** 439 (1976).
16. Goodman, D. W., Kelley, R. D., Madey, T. E., and Yates, J. T., Jr., *J. Catal.* **63,** 226 (1980).
17. Dwyer, D. J., and Somorjai, G. A., *J. Catal.* **52,** 291 (1978).
18. Krebs, H. J., and Bonzel, H. P., *Surf. Sci.* **99,** 570 (1980).
19. Bonzel, H. P., Krebs, H. J., and Schwarting, W., *Chem. Phys. Lett.* **72,** 165 (1980).
20. Brinen, J. S., and Malera, A., *J. Phys. Chem.* **76,** 2525 (1972).
21. Brinen, J. S., and Malera, A., *J. Catal.* **40,** 295 (1975).
22. Nefedov, V. I., *et al., Russ. J. Inorg. Chem.* **18,** 444 (1973).
23. (*a*) Castner, D. G., Sexton, B. A., and Somorjai, G. A., *Surf. Sci.* **71,** 519 (1978). (*b*) Dubois, L. H., and Somorjai, G. A., *Surf. Sci.* **91,** 514 (1980). (*c*) Castner, D. G., and Somorjai, G. A., *Surf. Sci.* **83,** 60 (1979).
24. Marbrow, R. A., and Lambert, R. M., *Surf. Sci.* **67,** 489 (1977).
25. (*a*) Thiel, P. A., Williams, E. D., Yates, J. T., and Weinberg, W. H., *Surf. Sci.* **84,** 54, 427 (1979). (*b*) Yates, J. T., Williams, E. D., and Weinberg, W. H., *Surf. Sci.* **91,** 562 (1980).
26. Campbell, C. T., and White, J. M., *J. Catal.* **54,** 289 (1978).
27. Castner, D. G., Dubois, L. H., Sexton, B. A., and Somorjai, G. A., *Surf. Sci.* **103,** L134 (1981).
28. Jarrell, M. S., and Gates, B., *J. Catal.* **40,** 255 (1975).
29. Christensen, B., and Scurrell, M. S., *J. Chem. Soc. Faraday Trans. 1* **74,** 2313 (1978).
30. Yashima, T., Orikasa, Y., Takahashi, N., and Hara, N., *J. Catal.* **59,** 53 (1979).
31. Kung, H. H., *Catal. Rev.* **22,** 235 (1980).
32. Poutsma, M. L., Elek, L. P., Ibarbia, P. A., Risch, A. P., and Rabo, J. A., *J. Catal.* **52,** 157 (1978).
33. Takeuchi, A., and Katzer, J. R., *J. Phys. Chem.* **85,** 937 (1981).
34. Ekerdt, J. G., and Bell, A. T., *J. Catal.* **62,** 19 (1980).
35. Rice, C. A., Worley, S. D., Curtis, C. W., Guin, J. A., and Tarrer, A. R., *J. Chem. Phys.* **74,** 6487 (1981).
36. Andersson, S. L. T., Watters, K. L., and Howe, R. F., *J. Catal.* **69,** 212 (1981).
37. Smith, A. K., Hagues, F., Theolier, A., Bassett, J. M., Ugo, R., Zonderighi, G. M., Bilhou, J. L., Bilhou-Bougnol, V., and Graydon, W. F., *Inorg. Chem.* **18,** 3104 (1979).